

Original Research

High Norepinephrine State Induces Growth of Colorectal Cancer Cells via ADP-Ribosyltransferase 1 in Type 2 Diabetes Mellitus

Wenwen Chen^{1,†}, Hailun Xie^{1,†}, Ming Xiao¹, Ming Li¹, Yi Tang¹, Shuxian Zhang¹,
Xiujun Li¹, Yalan Wang^{1,*}¹Department of Pathology, Molecular Medicine and Cancer Research Center, College of Basic Medicine, Chongqing Medical University, 400016 Chongqing, China*Correspondence: Wangyalan@cqmu.edu.cn (Yalan Wang)

†These authors contributed equally.

Academic Editor: Rajesh Katare

Submitted: 27 December 2022 Revised: 28 May 2023 Accepted: 15 June 2023 Published: 23 November 2023

Abstract

Background: Patients with type 2 diabetes mellitus have a higher susceptibility for colorectal cancer and poorer prognosis, but the mechanism is still unknown. Here, we investigated the effect of ADP-ribosyltransferase 1 (ART1) on the growth of colorectal cancer in an animal model of diabetes with high norepinephrine status, as well as the potential mechanism. **Methods:** We evaluated the size and weight of transplanted CT26 cell tumors with different ART1 expression levels in a mouse model of diabetes, as well as the survival time. CCK8 and flow cytometry were used to evaluate the growth of CT26 cells *in vitro*. Western blot was performed to analyze differentially expressed proteins in the ART1-modulated pathway. **Results:** High levels of norepinephrine and ART1 favored the proliferation of CT26 cells *in vitro* and *in vivo*. Moreover, inhibition of norepinephrine-dependent proliferation was observed in ART1-silenced CT26 cells compared to those with normal ART1 expression. Following reduction of the serum norepinephrine level by surgery, the size and weight of transplanted CT26 cell tumors was significantly reduced compared to non-operated and sham-operated mice. Furthermore, the expression of ART1, mTOR, STAT3, and p-AKT protein in the tumor tissue of diabetic mice was higher than in non-diabetic mice. Following reduction of the norepinephrine level by renal denervation (RD), expression of the proliferation-related proteins mTOR, STAT3, p-AKT protein decreased, but no change was seen for ART1 expression. At the same concentration of norepinephrine, ART1 induced the expression of p-AKT, mTOR, STAT3, CyclinD1 and c-myc in CT26 cells *in vitro*. **Conclusions:** We conclude that faster growth of colorectal cancer in high norepinephrine conditions requires the expression of ART1, and that high ART1 expression may be a novel target for the treatment of diabetes-associated colorectal cancer.

Keywords: ADP-ribosyltransferase 1; diabetes; norepinephrine; colorectal cancer; AKT

1. Introduction

Many studies to date have shown that type 2 diabetes mellitus (T2DM) is closely related to the occurrence and development of colorectal cancer (CRC). Compared with non-diabetic patients, T2DM patients have an increased risk of CRC and worse prognosis, although the specific mechanism is still unclear [1,2].

Insulin resistance (IR) is the pathophysiological basis of T2DM. IR activates the sympathetic nervous system (SNS), resulting in an increased level of circulating norepinephrine (NE) [3–5]. Long-term activation of the SNS leads to the onset of metabolic syndrome and increases the risk of T2DM, thus further aggravating IR and causing a vicious cycle [3,6–8]. A large number of studies indicate that NE activates the adrenergic receptor which in turn induces the cAMP-PKA, AKT-mTOR, ERK-Mnk1 and other signaling pathways. This subsequently affects the expression and activity of downstream molecules such as STAT3, c-myc and MMP-2, thereby affecting the biological behavior of tumor cells. The action of NE can be reduced by down-regulating its expression, or when the activity of

beta-adrenergic receptors on the surface of tumor cells is blocked by alpha/beta-receptor [9–17]. Therefore, a high level of NE-induced activation of signaling pathways such as AKT/mTOR/STAT3 may be a potential mechanism for the higher risk of CRC observed in patients with T2DM.

ADP-ribosyltransferase 1 (ART1) is an important mono-ADP ribose transferase that catalyzes post-translational modification of proteins by transferring a mono-ADP ribose to the protein target. ART1 is believed to have an important role in a variety of cellular biological properties [16,17]. We previously reported that changes in ART1 expression altered the phosphorylation level of AKT, as well as the activity and expression of mTOR, GSK-3 and c-myc. These subsequently affected the proliferation, invasion, metastasis, differentiation, angiogenesis and apoptosis of mouse CT26 CRC cells [18–20]. The AKT signaling pathway is one of the most important pathways involved in cell survival and insulin signaling [21]. Activation of AKT can promote the phosphorylation of mTOR, STAT3 and other downstream substrates to exert extensive biological effects, indicating that ART1 is



associated with glucose-related metabolic diseases. To our knowledge, the fundamental relationship between ART1 and the growth of CRC in conditions of T2DM and high NE status has yet to be reported.

In the present study, we investigated whether ART1 influences tumor growth and cell proliferation in an animal model of T2DM and CRC with high levels of NE. In addition, we explored whether the AKT/mTOR/STAT3 signaling pathway and the downstream molecules CyclinD1 and c-myc were involved in the mechanism, and whether there is crosstalk between ART1 and high NE status.

2. Materials and Methods

2.1 Cell Lines and Animals

The CT26 cell line was obtained from Professor YuQuan Wei (Sichuan University, Chengdu, Sichuan, China). ART1 short hairpin RNA (GFP-shRNA), ART1 over-expression (GFP-ART1) and vector control (GFP-Vector) CT26 cells were constructed [22,23]. Because NIH3T3 cell line is not reactive to NE according to previous reports [24], it was not set as control in the present study. All cell groups were cultured in RPMI-1640 medium (Hyclone, Logan, UT, USA) supplemented with 10% fetal bovine serum, 100 U/mL penicillin and 100 µg/mL streptomycin (Hyclone) at 37 °C in a 5% CO₂ incubator.

Balb/c mice (6–8 weeks old, 18–22 g) were obtained from the animal experiment center of Chongqing Medical University (Chongqing, China) and placed in a specific pathogen-free feeding room (20–26 °C, 12 h:12 h light-dark cycle). Mice were then randomly divided into two groups and fed either a normal-chow diet (NCD) or a high-fat diet (HFD). The NCD (catalog no. 5001, Research Diets Inc., New Brunswick, NJ, USA) provided 59% calories from carbohydrates, 20% from protein, and 19% from fat (14.61 KJ/g). The HFD (catalog no. 9398, Research Diets Inc) provided 30% of calories from carbohydrates, 18% from protein, and 50% from fat (19.75 KJ/g).

All experimental procedures were approved by the Animal Experimentation Ethics Committee (Chongqing Medical University) and were in accordance with the National Health and Medical Research Council of China Guidelines on Animal Experimentation. Mycoplasma testing has been done for the cell lines used in the research. Cell lines used have been authenticated by STR.

2.2 CT26 Cell Survival Assays and Flow Cytometry Analysis

CCK8 (CCK8 kit, Key Gen Biotechnology, Nanjing, PR China) assay was used to evaluate the effect of ART1 on the proliferation of CT26 cells in different concentrations of NE (0, 0.2, 0.4, 0.6, 0.8, 1.0 µM) for 24 h, or 1.0 µM of NE for different incubation times (12 h, 24 h, 36 h, 48 h). The absorbances (optical densities) were recorded with a universal microplate reader (Bio-Tek) at 450 nm. Assays were repeated at least three times.

Flow cytometry (Becton Dickinson Company, Franklin Lakes, NJ, USA) was used to evaluate the cell cycle distribution in each group treated with 1.0 µM NE for 48 h. All experiments were performed at least three times.

2.3 Establishment of Diabetic Mouse Model

A diabetic mouse model was established by feeding Balb/c mice with a HFD for six weeks and injecting with 1% streptozotocin (50 mg/kg, STZ, Sigma Chemical Co, St Louis, MO, USA) intraperitoneally. Control Balb/c mice fed a NCD were injected intraperitoneally with saline. Diabetes was defined as a random glucose concentration in tail vein blood of ≥ 11.1 mmol/L (test strips, Advantage, Bayer, Contour TS) one week after STZ injection [25–27].

2.4 Subcutaneous Tumor Transplant Model

Each experimental group consisted of 12 mice. The colorectal carcinoma complicated with diabetes mellitus (CRC/D) group (n = 48) was comprised of T2DM Balb/c mice fed the HFD. These were equally and randomly divided into the GFP-ART1 group (subcutaneously transplanted with GFP-ART1 CT26 cells), the GFP-shART1 group (GFP-shART1 CT26 cells), the non-transfection group (non-transfected CT26 cells), and GFP-Vector group (GFP-Vector CT26 cells). The colorectal carcinoma complicated with diabetes mellitus (CRC/D) group (n = 48) was comprised of Balb/c mice without T2DM and fed with NCD. These were also equally and randomly divided into GFP-ART1, GFP-shART1, non-transfected and GFP-Vector groups and subcutaneously transplanted with the appropriate CT26 cells as described above.

The CT26 cell suspension (2×10^6 /mL, 200 µL) was subcutaneously injected into the lateral skin of the right armpit of each mouse [28]. After 14 days, six mice were randomly selected from each group for sacrifice, and the weight and volume of the subcutaneous tumor was recorded. The survival time of the remaining mice in each group was recorded. Tumor volume was calculated according to the formula: volume = the maximum diameter \times the most trails² \times $\frac{1}{2}$ [29].

2.5 Renal Denervation (RD) and Sham Operation

Another 12 diabetic Balb/c mice inoculated with GFP-ART1 CT26 cells were equally divided into three groups: left RD (LRD, n = 4), left sham operation (LSO, n = 4), and no operation (GFP-ART1 group, n = 4). RD or sham surgery was performed as described previously [30,31]. In brief, mice were anaesthetized with an intraperitoneal ketamine injection (87 mg/kg). The kidneys were exposed by paravertebral line incision and the renal arteries and veins were isolated from connective tissue. After stripping the visible nerves, the vessels were painted for 2 minutes with a solution of 10% phenol in absolute ethanol. The muscular layers of the abdominal wall were sutured with absorp-

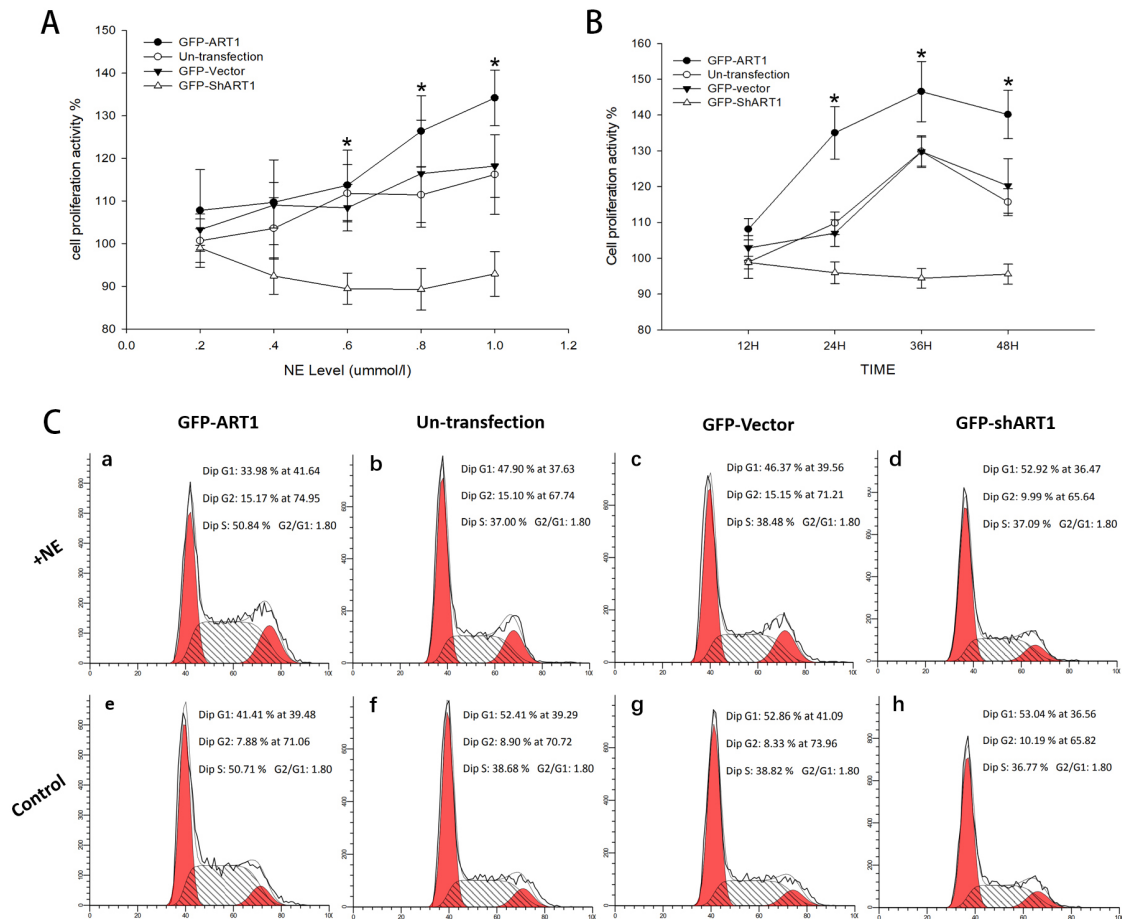


Fig. 1. High concentrations of NE induce ART1-dependent proliferation in CT26 cells. (A) Proliferation of CT26 cells with different ART1 expression levels after treatment with different concentrations of NE. (B) Proliferation of CT26 cells with different ART1 expression levels and treated with 1 $\mu\text{mol/L}$ NE for different times. (C) Cell cycle distribution of CT26 cells with different ART1 expression levels and treated with or without NE. (a) GFP-ART1 CT26 cells treated with 1 $\mu\text{mol/L}$ NE. (b) Non-transfected CT26 cells treated with 1 $\mu\text{mol/L}$ NE. (c) GFP-Vector CT26 treated with 1 $\mu\text{mol/L}$ NE. (d) GFP-shART1 CT26 cells treated with 1 $\mu\text{mol/L}$ NE. (e) GFP-ART1 CT26 cells with no NE treatment. (f) Non-transfected CT26 cells with no NE treatment. (g) GFP-Vector CT26 cells with no NE treatment. (h) GFP-shART1 CT26 cells with no NE treatment. NE, norepinephrine.

tive material and the skin was closed by non-absorptive filament. Animals recovered from anesthesia within 10–20 minutes after the end of surgery. In the sham operation, the renal nerves were isolated but preserved. As described earlier [31], successful denervation was assessed by measuring the renal tissue content of catecholamines using an enzyme-linked immunosorbent assay (ELISA) KIT (Cloud-Clone, Houston, TX, USA). Completeness of denervation was assumed when the NE tissue content was <10% of the mean value observed in the sham-operated group [30].

The day after operation, all mice were inoculated with GFP-ART1 CT26 cells in the right axillary fossa. The mice were killed after two weeks and the kidneys and transplanted tumor were excised. These were weighed and the tumor volume measured, then stored frozen in liquid nitrogen. Blood was also obtained from each animal.

2.6 Western Blot Analyses

CT26 cells and Balb/c mice transplant tumors were placed in lysis buffer (Beyotime, Shanghai, China) and the proteins electrophoresed on SDS-PAGE gel and transferred to PVDF membranes. The membranes were blocked with 5% nonfat dried milk and incubated overnight at 4 $^{\circ}\text{C}$ with primary antibodies against ART1 (Abgent, San Diego, CA, USA; 1:500 dilution), Akt kinase (Akt), phospho-Akt (p-AKT), STAT3, mTOR, CyclinD1, and c-myc (Cell Signaling Technology, MA, USA; 1:1000 dilution). They were then incubated with horseradish peroxidase-conjugated secondary antibody at a dilution of 1:1000 (ZSGBBIO, Beijing, China). Finally, the membranes were assessed using enhanced chemiluminescence reagents (Beyotime) and analyzed with Quantity One software (BioRad Laboratories, Hercules, CA, USA). Betaactin was used as a loading control for the western blotting experiments.

Table 1. Cell cycle distribution and proliferation indices (PI) of CT26 cells in different ART1 groups ($\bar{x} \pm SD$).

Group	Cell cycle distribution			PI (%)
	G1 phase	S phase	G2 phase	(G2 + S)/(G1 + S + G2)
GFP-ART1 + NE	34.75 ± 0.78***▲▲	51.96 ± 0.52***▲▲	13.30 ± 0.57	65.25 ± 0.78***▲▲
Non-transfection + NE	45.25 ± 0.58**	42.45 ± 1.88*	12.30 ± 1.46	54.75 ± 0.58**
GFP-Vector + NE	45.55 ± 0.50**	41.45 ± 1.33	13.00 ± 1.06	54.45 ± 0.50**
GFP-shART1 + NE	56.47 ± 1.17##	31.08 ± 1.62##	12.45 ± 0.77	43.53 ± 1.17##
GFP-ART1	40.52 ± 0.57***▲▲	47.84 ± 1.30***▲▲	11.64 ± 1.17	59.48 ± 0.57***▲▲
Non-transfection	51.05 ± 0.63	34.83 ± 1.86	14.12 ± 1.54	48.95 ± 0.63
GFP-Vector	50.97 ± 0.7	37.35 ± 1.77	11.69 ± 1.52	49.03 ± 0.70
GFP-shART1	57.65 ± 1.53##	29.85 ± 1.51#	12.50 ± 1.24	42.36 ± 1.53##

Each CT26 + NE vs. each CT26: * $p < 0.05$ ** $p < 0.01$;

GFP-ART1 + NE vs. Non-transfection + NE, GFP-shART1 + NE vs. GFP-Vector + NE: # $p < 0.05$ ## $p < 0.01$;

GFP-ART1 + NE vs. GFP-shART1 + NE: ▲▲ $p < 0.01$;

GFP-ART1 vs. Non-transfection, GFP-shART1 vs. GFP-Vector: # $p < 0.05$ ## $p < 0.01$; GFP-ART1 vs. GFP-shART1: ▲▲ $p < 0.01$.

Table 2. Effect of ART1 on the proliferation of mouse colon carcinoma CT26 cells treated with different concentrations of NE ($\bar{x} \pm SD$).

NE ($\mu\text{mol/L}$)	GFP-ART1	Non-transfection	GFP-vector	GFP-shART1
0.2	107.79 ± 9.56	100.68 ± 5.12	103.28 ± 3.68	98.97 ± 4.51
0.4	109.70 ± 9.94	103.59 ± 7.20	109.04 ± 5.34	92.41 ± 4.26
0.6	113.69 ± 8.23##	111.80 ± 6.71	108.41 ± 5.47	89.44 ± 3.64*
0.8	126.36 ± 8.32##	111.43 ± 6.55	116.42 ± 12.53	89.27 ± 4.86*
1.0	134.16 ± 6.53##*	116.20 ± 9.36	118.21 ± 7.33	92.91 ± 5.24*

GFP-ART1 vs. GFP-shART1: ## $p < 0.01$;

GFP-ART1 vs. Non-transfection, GFP-vector vs. GFP-shART1: * $p < 0.05$.

Table 3. ART1 affects the proliferation of CT26 cells treated with 1.0 μM NE for different durations ($\bar{x} \pm SD$).

Time (h)	GFP-ART1	Non-transfection	GFP-vector	GFP-shART1
12	108.12 ± 2.99	98.93 ± 4.56	102.88 ± 3.44	98.81 ± 1.77
24	135.04 ± 7.32##**	109.80 ± 3.15	107.01 ± 3.71	95.97 ± 3.02
36	146.55 ± 8.40##*	129.82 ± 4.39	129.78 ± 4.03	94.41 ± 2.72**
48	140.13 ± 6.77##**	115.72 ± 3.77	120.24 ± 7.61	95.56 ± 2.78**

GFP-ART1 vs. GFP-shART1: ## $p < 0.01$;

GFP-ART1 vs. Non-transfection, GFP-vector vs. GFP-shART1: * $p < 0.05$, ** $p < 0.01$.

2.7 Evaluation of Serum Insulin and NE Levels

Serum levels of insulin and NE were measured using commercial enzyme-linked immunosorbent assay kits (Cloud-Clone) according to the manual.

2.8 Statistical Analysis

Data was analyzed using the SPSS 19.0 statistical software package (SPSS, Chicago, IL, USA). Numerical data were compared using the chi-square test. Binary logistic regression was used to analyze T2DM and ART1 expression in CRC patients. All values shown are the mean \pm standard error of the mean (SEM). Unpaired Student t -test was used for two-group comparisons. One-way ANOVA was used for intra-group comparisons, followed by a least significant difference post hoc test to compare between groups. $p < 0.05$ was considered as statistically significant.

3. Results

3.1 High Concentrations of NE Boost the Proliferation of CT26 Cells and Requires ART1

CT26 cells from GFP-ART1, non-transfection, GFP-Vector and GFP-ShART1 groups were induced for 24 h with 0.2, 0.4, 0.6, 0.8 and 1 μM NE concentrations. With increasing concentrations of NE, cell proliferation was observed to gradually increase in the CT26 cell groups expressing ART1 (GFP-ART1, non-transfection and GFP-Vector groups), but not in ART1-silenced CT26 cells (Fig. 1A). We further studied the time-dependence of NE on cell proliferation in the four experimental groups. Each group was treated with 1 μM NE for 12, 24, 36 and 48 h. Cell proliferation was found to increase progressively from 12 h to 36 h in the GFP-ART1, non-transfection and GFP-Vector groups, and then decreased after 48 h treat-

Table 4. Weight of Balb/C mice after transplantation with different CT26 cells ($\bar{x} \pm SD$).

Group	CRCD weight loss (g)	CRCO weight loss (g)
GFP-ART1	8.54 ± 0.33***▲▲	6.37 ± 0.32***▲▲
Non-transfection	8.16 ± 0.41**	5.27 ± 0.61
GFP-vector	7.94 ± 0.38**	5.64 ± 0.47
GFP-shART1	7.4 ± 0.38***	4.82 ± 0.55**

CRCD vs. CRCO at different ART1 expression levels: ** $p < 0.01$; CRCD group: GFP-ART1 vs. Non-transfection, GFP-shART1 vs. GFP-Vector, # $p < 0.05$, ## $p < 0.01$; GFP-ART1 vs. GFP-shART1: ▲▲ $p < 0.01$; CRCO group: GFP-ART1 vs. Non-transfection, GFP-shART1 vs. GFP-Vector, # $p < 0.05$, ## $p < 0.01$; GFP-ART1 vs. GFP-shART1: ▲▲ $p < 0.01$.

ment. However, no significant increase with treatment time was observed in the GFP-ShART1 group (Fig. 1B). Flow cytometry showed a decreased percentage of G1 phase and increased S phase and proliferation indices (PI) in the GFP-ART1 group compared to the non-transfection and GFP-Vector groups. In contrast, the GFP-shART1 group had an increased percentage of G1 phase and decreased S phase and PI. Following NE induction, CT26 cells that expressed ATR1 (GFP-ART1, non-transfection and GFP-Vector groups) showed a decreased percentage of G1 phase cells and increased percentage of S phase and PI cells. In contrast, ATR1-silenced CT26 cells showed no obvious difference in cell cycle distribution or PI (Fig. 1C, Table 1). Together, these results suggest that a high concentration of NE and an appropriate treatment time can induce ART1-dependent proliferation of CT26 cells.

At the same NE concentration and treatment time, the proliferation of CT26 cells was highest in the GFP-ART1 group and lowest in the GFP-ShART1 group (Tables 2,3), thus demonstrating that ART1 boosts the proliferation of CT26 cells.

3.2 Establishment of Animal Model of Diabetes

A diabetic Balb/c mouse model was established by feeding a HFD and intraperitoneal injection with 1% STZ. Blood tests showed significantly higher glucose concentrations, insulin levels and NE levels in diabetic mice compared to mice fed an NCD. Diabetic mice also had higher weight (Fig. 2). These results demonstrate successful establishment of the Balb/c mouse diabetic model.

Diabetic mice were inoculated with CT26 cells subcutaneously into the right axillary fossa. Following inoculation with cells having the same ART1 expression level, diabetic mice lost more weight than non-diabetic mice ($p < 0.01$). However, the absolute value of body weight was still higher in the CRCD group compared to the CRCO group (21.82 ± 1.64 vs. 21.04 ± 1.08 g, respectively, $p < 0.05$) (Table 4). Moreover, both the volume and weight of transplanted tumors in the CRCD group were higher than

Table 5. Effect of ART1 expression on the weight of transplanted tumors in Balb/C mice ($\bar{x} \pm SD$).

Group	CRCD weight (g)	CRCO weight (g)
GFP-ART1	6.85 ± 0.37***▲▲	3.44 ± 0.65***▲▲
Non-transfection	3.3 ± 0.28**	1.89 ± 0.29
GFP-vector	3.7 ± 0.47**	1.77 ± 0.19
GFP-shART1	2.17 ± 0.26***	0.6 ± 0.19#

CRCD vs. CRCO at different ART1 expression levels: ** $p < 0.01$; CRCD group: GFP-ART1 vs. Non-transfection, GFP-shART1 vs. GFP-Vector: # $p < 0.05$, ## $p < 0.01$; GFP-ART1 vs. GFP-shART1: ▲▲ $p < 0.01$; CRCO group: GFP-ART1 vs. Non-transfection, GFP-shART1 vs. GFP-Vector: # $p < 0.05$, ## $p < 0.01$; GFP-ART1 vs. GFP-shART1: ▲▲ $p < 0.01$.

Table 6. Effect of ART1 expression on the volume of transplanted tumors in Balb/C mice ($\bar{x} \pm SD$).

Group	CRCD(V)/cm ³	CRCO(V)/cm ³
GFP-ART1	6.48 ± 0.7***▲▲	2.59 ± 0.17***▲▲
Non-transfection	2.9 ± 0.64*	1.34 ± 0.1
GFP-vector	3.83 ± 0.42**	1.7 ± 0.29
GFP-shART1	1.99 ± 0.33**	0.4 ± 0.17**

CRCD vs. CRCO in different ART1 expression level: ** $p < 0.01$; CRCD group: GFP-ART1 vs. Un-transfection, GFP-shART1 vs. GFP-Vector: # $p < 0.05$, ## $p < 0.01$; GFP-ART1 vs. GFP-shART1: ▲▲ $p < 0.01$; CRCO group: GFP-ART1 vs. Un-transfection, GFP-shART1 vs. GFP-Vector: # $p < 0.05$, ## $p < 0.01$; GFP-ART1 vs. GFP-shART1: ▲▲ $p < 0.01$.

in the CRCO group ($p < 0.05$). Mice injected with high ART1 expressing CT26 cells showed the most body weight loss (8.54 ± 0.33 g) and the largest and heaviest tumors ($p < 0.01$), whereas mice injected with ATR1-silenced CT26 cells had the least body weight loss (4.82 ± 0.55 g) and the smallest and lightest transplanted tumors (Fig. 3A,B; Tables 5,6).

3.3 ART1 Impacts the Growth of Transplanted Tumor Cells and the Survival Time of Both Diabetic and Non-Diabetic Mice

We also investigated the effect of ART1 expression and diabetes on the survival of mice with CT26 tumor cell transplants. Following inoculation with CT26 cells expressing the same level of ART1, the survival of CRCD mice was shorter than that of CRCO mice ($p < 0.05$) (Fig. 3C). Furthermore, the survival of both CRCD and CRCO mice was shortest in those injected with high ART1 expressing CT26 cells, and longest in those injected with ATR1-silenced CT26 cells ($p < 0.01$) (Table 7).

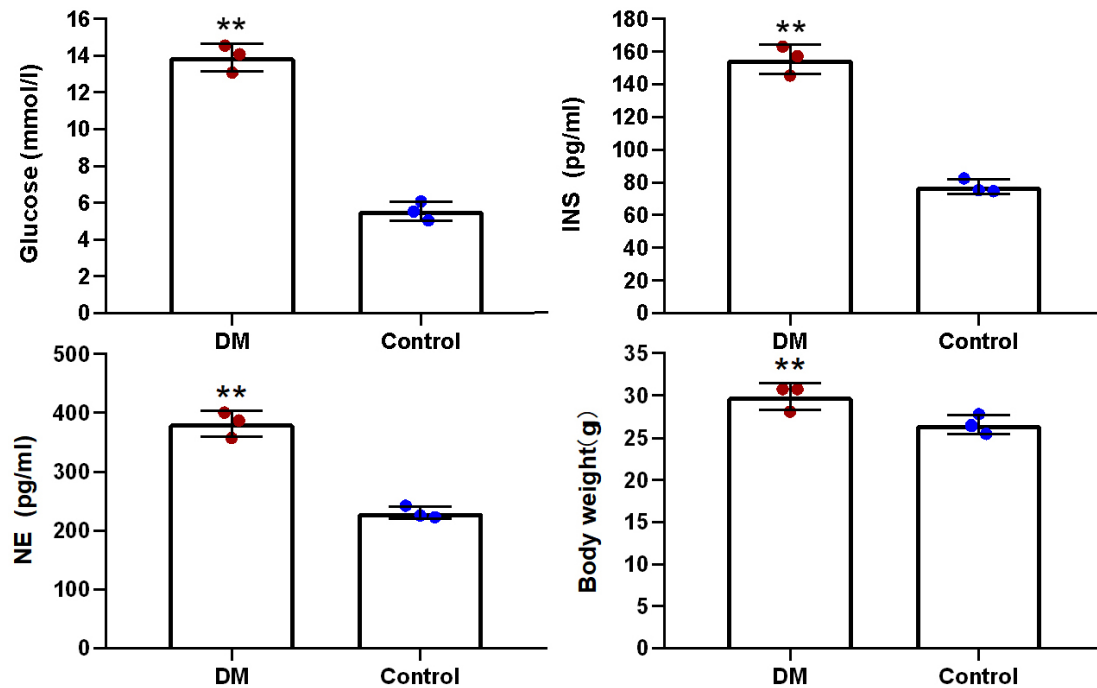


Fig. 2. Metabolic index of DM mice and of non-DM mice (** $p < 0.01$). DM, diabetes mellitus.

Table 7. Survival of Balb/C mice after transplantation with different ART1 expressing CT26 cells ($\bar{x} \pm SD$).

Group	CRCD survival time (days)	CRCO survival time (days)
GFP-ART1	15.67 \pm 1.26 ^{##▲▲}	18.5 \pm 0.56 ^{##▲▲}
Non-transfection	24.17 \pm 0.98	27.5 \pm 1.2
GFP-vector	23.83 \pm 1.62	27.17 \pm 1.14
GFP-shART1	34.17 \pm 1.83 ^{###}	39.5 \pm 1.36 ^{##}

CRCD vs. CRCO at different ART1 expression levels: * $p < 0.05$;

CRCD group: GFP-ART1 vs. Non-transfection, GFP-shART1 vs. GFP-Vector:

^{###} $p < 0.01$; GFP-ART1 vs. GFP-shART1: ^{▲▲} $p < 0.01$;

CRCO group: GFP-ART1 vs. Non-transfection, GFP-shART1 vs. GFP-Vector:

^{###} $p < 0.01$; GFP-ART1 vs. GFP-shART1: ^{▲▲} $p < 0.01$.

3.4 Renal Denervation Reduces the Level of Blood Glucose and the Growth of Tumor Cell Transplants with High ART1 Expression in CRCD Mice

Animal models of RD were successfully established, with the NE level reduced by $>10\%$ in the kidney and plasma of the operated group (LRD) ($p < 0.01$) [30,31]. The blood glucose and plasma insulin levels of each group were also measured, together with the volume and weight of transplanted tumor. The results showed lower blood glucose and plasma insulin levels, and smaller and lighter tumors in the LRD group compared with the sham-operated (LSO) and non-operated groups ($p < 0.01$). No significant differences were observed between the non-operated and LSO groups ($p > 0.05$) (Fig. 4; Tables 8,9).

3.5 ART1 is Positively Associated with the Expression of p-AKT, mTOR, STAT3, cyclinD1 and c-myc in CT26 Cells Induced by High NE

GFP-ART1 CT26 cells showed the highest levels of protein expression for ART1, p-AKT, mTOR, STAT3, CyclinD1 and c-myc ($p < 0.01$). In contrast, GFP-shART1 CT26 cells showed the lowest expression of these protein markers ($p < 0.01$), suggesting that ART1 contributes to the up-regulation of p-AKT, mTOR, STAT3, CyclinD1 and c-myc in cells with high NE (Fig. 5A).

3.6 Expression of ART1, p-AKT, mTOR and STAT3 in Transplanted Tumors from CRCD and CRCO Mice, and Changes after Renal Denervation in the CRCD Group

The expression of ART1, mTOR and STAT3 was significantly higher in CRCD mice compared with CRCO mice ($p < 0.01$). Although there was no difference in the expression of AKT ($p > 0.05$), the expression of p-AKT was significantly higher in CRCD mice compared

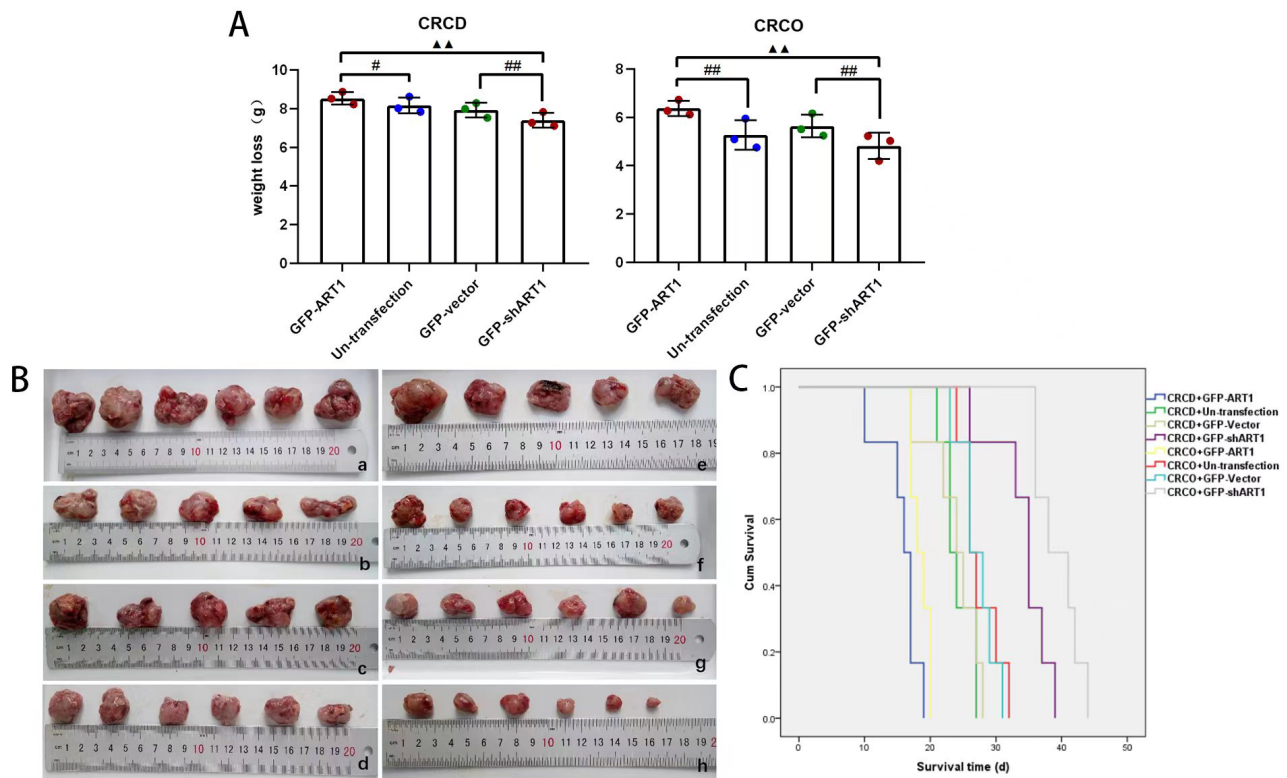


Fig. 3. ART1 increases the growth of transplanted tumor while reduce the survival time of both CRCD and CRCO mice. (A) shows the results for DM mice transplanted with CT26 cells expressing different levels of ART1 and the results for non-DM mice transplanted with CT26 cells expressing different levels of ART1 (GFP-ART1 vs. Non-transfected, GFP-shART1 vs. GFP-Vector, $^{\#}p < 0.05$ $^{\#\#}p < 0.01$; GFP-ART1 vs GFP-shART1: $^{\blacktriangle\blacktriangle}p < 0.01$), respectively. (B) Tumor size in DM mice and in non-DM mice transplanted with CT26 cells expressing different levels of ART1. (a) DM mice transplanted with GFP-ART1 CT26 cells. (b) DM mice transplanted with non-transfected CT26 cells. (c) DM mice transplanted with GFP-Vector CT26 cells. (d) DM mice transplanted with GFP-shART1 CT26 cells. (e) Non-DM mice transplanted with GFP-ART1 CT26 cells. (f) Non-DM mice transplanted with non-transfected CT26 cells. (g) Non-DM mice transplanted with GFP-Vector CT26 cells. (h) Non-DM mice transplanted with GFP-shART1 CT26 cells. (C) Survival curves for DM mice and non-DM mice transplanted with CT26 cells expressing different levels of ART1.

with CRCO mice ($p < 0.01$) (Fig. 5B). *In vivo* data also revealed that a high-NE environment boosted the expression of ART1, as well as p-AKT, mTOR and STAT3.

To investigate the effect of NE on the ART1-dependent proliferation of CT26 cells, GFP-ART1 CT26 cells were inoculated in the non-surgery group, LSO group (sham operation) and LRD group (renal denervation). No significant differences in ART1 and AKT protein expression were found between the three groups ($p > 0.05$). However, the expression of p-AKT ($p < 0.01$), mTOR ($p < 0.05$) and STAT3 ($p < 0.05$) proteins was clearly lower in the LRD group compared to the non-surgery and LSO groups (Fig. 5C). This suggests that NE deprivation leads to a consistent decrease in p-AKT, mTOR and STAT3 expression. Interestingly, however, the ART1 and AKT levels did not decrease, suggesting that even if NE affects the expression of proliferation-related proteins, the expression of ART1 itself is not dependent on the NE level.

4. Discussion

Epidemiological studies and bioinformatic analyses have found that T2DM is a risk factor for CRC, as well as being a prognostic factor for adverse survival outcomes in such patients [1,2]. T2DM is a metabolic disease characterized by IR, hyperinsulinemia, chronic activation of the SNS, increased circulating NE levels, and a high NE status [3,6–8]. Increased NE levels have been reported to promote CRC liver metastasis, possibly through the beta-adrenergic receptor signaling pathway [32]. Large case-control studies have also found that long-term use of NE antagonists or beta-receptor blocking agents can reduce the risk of malignant tumors, including CRC [14,15,33]. Therefore, high levels of NE are likely to be related to CRC development in addition to T2DM.

In the present study, ART1 was found to be necessary for the proliferation of CRC cells in a high-NE environment accompanied with diabetes. Our further research revealed

Table 8. Biochemical characteristics after renal denervation ($\bar{x} \pm SD$).

Group	Kidney NE (ng/g)	Plasma NE (pg/mL)	Glucose (mmol/L)	Fins (pg/mL)
Non-operated group	499.96 \pm 14.83**	466.06 \pm 13.52**	14.08 \pm 0.19**	175.57 \pm 3.72**
LSO	510.74 \pm 15.4**	452.37 \pm 7.01**	13.7 \pm 0.15**	178.94 \pm 2.7**
LRD	169.19 \pm 4.74	211.73 \pm 2.61	11.97 \pm 0.15	130.12 \pm 3.88

Non-operated group vs. LRD, LSO vs. LRD: ** $p < 0.01$.

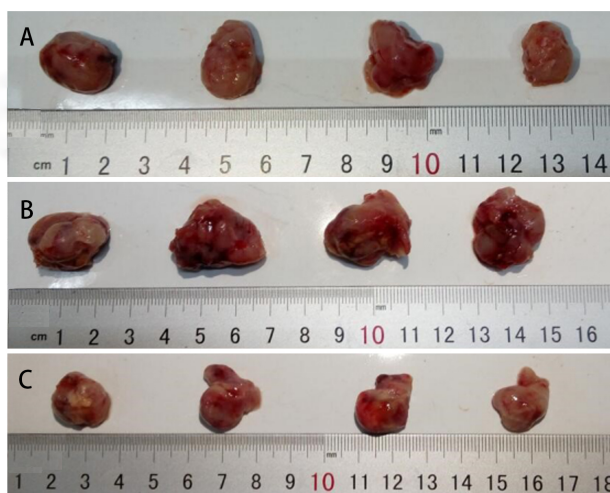


Fig. 4. Tumor size in DM mice transplanted with CT26 cells expressing high levels of ART1 and surgical intervention to alter the serum NE level. (A) GFP-ART1 group. (B) LSO group. (C) LRD group.

that ART1 activated the AKT-mTOR pathway, resulting in increased STAT3 phosphorylation and ultimately promoting Cyclin D1 and c-myc expression and cell proliferation.

Our previous studies [18–20,22] showed that high ART1 expression boosted the malignant biological behavior of CRC, and that ADP-ribosylation could affect glucose metabolism via several pathway [34]. However, so far there has been no research on the effect of ART1 on CRC associated with diabetes mellitus. Therefore, in the present study we investigated the effect of changes in ART1 expression on CRC associated with T2DM. Regardless of whether mice were fed a normal or HFD, elevated ART1 expression was observed more often in those with lymph node metastasis than those without. This confirms the results of our previous study and suggests that ART1 expression is related to the malignant behavior of CRC. Importantly, mice fed a HFD had higher expression of ART1 compared to mice fed a normal diet. These results suggest that ART1 expression may be related to CRC-associated disorders of glucose metabolism, but the mechanism underlying this association remains to be clarified.

In vivo experiments showed that diabetes was a positive factor for the growth of CRC tumor cell transplants when ART1 expression was constant. Furthermore, increased ART1 expression accelerated the growth of these

Table 9. Effect of NE level on transplanted tumor weight and volume after renal denervation ($\bar{x} \pm SD$).

Group	Volume (cm ³)	Weight (g)
Non-operated group	2.08 \pm 0.5**	3.73 \pm 0.35**
LSO	2.1 \pm 0.5**	3.75 \pm 0.39**
LRD	0.56 \pm 0.19	2.1 \pm 0.36

Non-operated group vs. LRD, LSO vs. LRD: ** $p < 0.01$.

tumors and shortened the survival time in both the diabetic and non-diabetic mouse models. Thus, both diabetes and ART1 encouraged the growth of xenografts. However, diabetic and non-diabetic mice still showed a difference in xenograft growth when ART1 was silenced, suggesting the diabetes-accelerated growth of xenografts was not due entirely to ART1.

The *in vitro* study conducted here also showed that CT26 cells with high ART1 expression showed consistently higher proliferation rates with increasing NE concentrations and induction times. However, no significant changes were detected in the proliferation of ART1-silenced CT26 cells following increases in NE concentration and induction time. These results highlight that NE-promoted proliferation of CRC CT26 cells is dependent on ART1. Although the diabetes-accelerated growth of xenografts was not totally dependent on ART1, we conclude from our findings that NE promotion of CRC cell proliferation is dependent on ART1.

Phosphorylated STAT3 is linked to the activation of Akt/mTOR, with this pathway being involved in cell proliferation and growth. Results from both *in vitro* and *in vivo* experiments have shown that ART1 expression in a high NE environment is positively associated with the expression of p-AKT, mTOR and STAT3, but not AKT. Following LRD-induced reduction in the blood level of NE, the expression of p-AKT, mTOR and STAT3 protein in transplanted tumor cells decreased significantly, whereas no change was observed in the expression of ART1 and AKT protein. Moreover, the volume and weight of the transplanted tumor also decreased significantly, thus confirming that reduction of the NE level is an effective strategy for inhibiting xenograft growth. Consistent with our observations, Lima-Seolin *et al.* [35] also found increased activity of the AKT/mTOR/STAT3 signaling pathway in high NE conditions. Our results suggest that NE is not required for ART1 expression, but is required for ART1-induced activation of the AKT/mTOR/STAT3 signaling pathway.

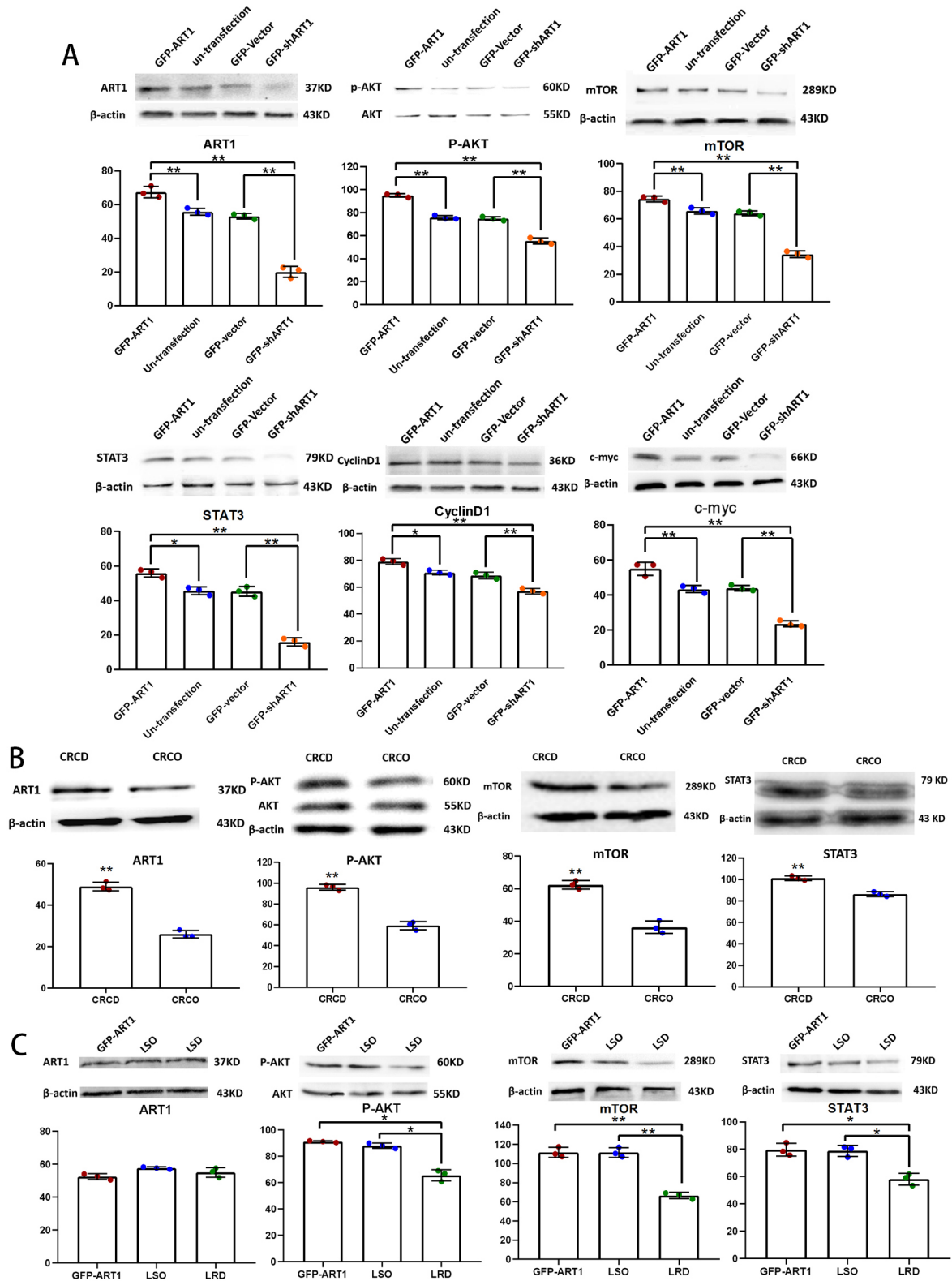


Fig. 5. ART1 contributes to the up-regulation of p-AKT, mTOR, STAT3, CyclinD1 and c-myc in CT26 cells with high NE level. (A) ART1, p-AKT, mTOR, STAT3, cyclinD1 and c-myc expression in each CT26 cell group treated with 1 $\mu\text{mol/L}$ NE (** $p < 0.01$; * $p < 0.05$). (B) ART1, p-AKT, mTOR, and STAT3 expression in transplanted CT26 cells in a balb/c mouse model of diabetes mellitus. CRCD: colorectal carcinoma associated with diabetes mellitus; CRCO: colorectal carcinoma not associated with diabetes mellitus (** $p < 0.01$). (C) Effect of renal denervation on ART1, p-AKT, mTOR, STAT3 expression in three experimental groups with transplanted tumor cells (** $p < 0.01$; * $p < 0.05$).

STAT3 can increase the transcription of CyclinD1 and c-myc, thus promoting the indefinite proliferation of cells. Our results indicated that expression of ART1 up-regulated the expression of CyclinD1 and c-myc proteins in conditions of high NE. Together with previous results, we hypothesize that ART1 up-regulates the expression of CyclinD1 and c-myc proteins in high NE conditions by activating the AKT/mTOR/STAT3 signal pathway, thereby promoting the proliferation and growth of CT26 cells.

A recent study used TaqMan OpenArray panels to analyze gene expression patterns in colon carcinoma samples from T2DM and non-diabetic patients [36]. This revealed that T2DM impacts CRC mainly through five pathways, namely Wnt (wingless-type)/ β -catenin, Hippo, TNF, PI3K/Akt, and platelet activation, thus partially confirming the results of the present study.

5. Limitation

In this present study we applied long term high-fat diet combined with low-dose STZ injection to simulate the insulin resistance state of T2DM to the greatest extent [37–39]. In view of the tolerance of the mouse model to the subsequent two surgeries (renal sympathetic denervation and subcutaneous tumor transplantation), we chose Blab/c mice instead of nude mice for the experiment, and therefore accordingly we did not use human colorectal cancer cell lines. That is a limitation for our study. It's worth seeking a mouse model compatible with human CRC cells for further validation of our findings in next step of research.

6. Conclusions

In conclusion, we hypothesize that ART1 plays an important role in stimulating the proliferation of CRC cells under high NE conditions. The specific mechanism is likely to include activation of the AKT/mTOR/STAT3 pathway, thereby up-regulating the expression of Cyclin D1 and c-myc protein and subsequently promoting the growth of CRC. Although the molecular mechanisms require further clarification, our results may provide an explanation for the poorer prognosis of CRC patients with T2DM and high NE status compared to non-diabetic patients. Moreover, these results suggest that ART1 could be used as a therapeutic target in CRC patients with T2DM.

Consent for Publication

Not applicable.

Availability of Data and Materials

Data supporting the findings of this study are available upon reasonable request to the corresponding author.

Author Contributions

WWC established the animal modules, obtained samples from mice and was a major contributor to writing the

manuscript. HLX and ML performed Western blot for cells and tissue samples. MX conducted the animal experiments and was a contributor to writing the manuscript. YT and SXZ performed the CT26 cell survival assay and flow cytometry. HLX and XJL contributed to the animal experiments. YLW analyzed the data and was contributor in writing the manuscript. All authors read and approved the final manuscript. All authors have participated sufficiently in the work and agreed to be accountable for all aspects of the work.

Ethics Approval and Consent to Participate

All animal experiments were approved and performed in accordance with the guidelines and regulations of the Institutional Animal Care and Ethics Committee of Chongqing Medical University (Reference No.: 0002675).

Acknowledgment

The authors thank all current and past members of the Department of Pathology, Chongqing Medical University.

Funding

This research was supported by the Science and Technology Research Foundation of the Chongqing Municipal Education Commission (KJQN201800435), and the Innovation Project for Graduate Students in Chongqing (CYB19160).

Conflict of Interest

The authors declare no conflict of interest.

Supplementary Material

Supplementary material associated with this article can be found, in the online version, at <https://doi.org/10.31083/j.fbl2811295>.

References

- [1] Yuan C, Zhang X, Babic A, Morales-Oyarvide V, Zhang Y, Smith-Warner SA, *et al.* Preexisting Type 2 Diabetes and Survival among Patients with Colorectal Cancer. *Cancer Epidemiology, Biomarkers & Prevention*. 2021; 30: 757–764.
- [2] Ottaiano A, Circelli L, Santorsola M, Savarese G, Fontanella D, Gigantino V, *et al.* Metastatic colorectal cancer and type 2 diabetes: prognostic and genetic interactions. *Molecular Oncology*. 2022; 16: 319–332.
- [3] Huggett RJ, Scott EM, Gilbey SG, Stoker JB, Mackintosh AF, Mary DASG. Impact of type 2 diabetes mellitus on sympathetic neural mechanisms in hypertension. *Circulation*. 2003; 108: 3097–3101.
- [4] Boulton AJM, Vinik AI, Arezzo JC, Bril V, Feldman EL, Freeman R, *et al.* Diabetic neuropathies: a statement by the American Diabetes Association. *Diabetes Care*. 2005; 28: 956–962.
- [5] Stein PK, Barzilay JI, Domitrovich PP, Chaves PM, Gottdiener JS, Heckbert SR, *et al.* The relationship of heart rate and heart rate variability to non-diabetic fasting glucose levels and the metabolic syndrome: the Cardiovascular Health Study. *Diabetic Medicine*. 2007; 24: 855–863.
- [6] Mancia G, Bousquet P, Elghozi JL, Esler M, Grassi G, Julius S,

- et al.* The sympathetic nervous system and the metabolic syndrome. *Journal of Hypertension*. 2007; 25: 909–920.
- [7] Grassi G, Dell'oro R, Quarti-Trevano F, Scopelliti F, Seravalle G, Palermi F, *et al.* Neuroadrenergic and reflex abnormalities in patients with metabolic syndrome. *Diabetologia*. 2005; 48:1359–1365.
- [8] Huggett RJ, Burns J, Mackintosh AF, Mary DASG. Sympathetic neural activation in nondiabetic metabolic syndrome and its further augmentation by hypertension. *Hypertension*. 2004; 44: 847–852.
- [9] Yang EV, Sood AK, Chen M, Li Y, Eubank TD, Marsh CB, *et al.* Norepinephrine up-regulates the expression of vascular endothelial growth factor, matrix metalloproteinase (MMP)-2, and MMP-9 in nasopharyngeal carcinoma tumor cells. *Cancer Research*. 2006; 66: 10357–10364.
- [10] Sood AK, Bhatta R, Kamat AA, Landen CN, Han L, Thaker PH, *et al.* Stress hormone-mediated invasion of ovarian cancer cells. *Clinical Cancer Research*. 2006; 12: 369–375.
- [11] Landen CN, Jr, Lin YG, Armaiz Pena GN, Das PD, Arevalo JM, Kamat AA, *et al.* Neuroendocrine modulation of signal transducer and activator of transcription-3 in ovarian cancer. *Cancer Research*. 2007; 67: 10389–10396.
- [12] Huang XY, Wang HC, Yuan Z, Huang J, Zheng Q. Norepinephrine stimulates pancreatic cancer cell proliferation, migration and invasion via β -adrenergic receptor-dependent activation of P38/MAPK pathway. *Hepato-Gastroenterology*. 2012; 59: 889–893.
- [13] Deng GH, Liu J, Zhang J, Wang Y, Peng XC, Wei YQ, *et al.* Exogenous norepinephrine attenuates the efficacy of sunitinib in a mouse cancer model. *Journal of Experimental & Clinical Cancer Research*. 2014; 33: 21.
- [14] Friedman GD, Udaltsova N, Habel LA. Norepinephrine antagonists and cancer risk. *International Journal of Cancer*. 2011; 128: 737–738; author reply 739.
- [15] Fitzgerald PJ. Is norepinephrine an etiological factor in some types of cancer? *International Journal of Cancer*. 2009; 124: 257–263.
- [16] Laing S, Unger M, Koch-Nolte F, Haag F. ADP-ribosylation of arginine. *Amino Acids*. 2011; 41: 257–269.
- [17] Okazaki IJ, Moss J. Mono-ADP-ribosylation: a reversible post-translational modification of proteins. *Advances in Pharmacology*. 1996; 35: 247–280.
- [18] Xu JX, Xiong W, Zeng Z, Tang Y, Wang YL, Xiao M, *et al.* Effect of ART1 on the proliferation and migration of mouse colon carcinoma CT26 cells in vivo. *Molecular Medicine Reports*. 2017; 15: 1222–1228.
- [19] Yang L, Xiao M, Li X, Tang Y, Wang YL. Arginine ADP-ribosyltransferase 1 promotes angiogenesis in colorectal cancer via the PI3K/Akt pathway. *International Journal of Molecular Medicine*. 2016; 37: 734–742.
- [20] Xiao M, Tang Y, Wang YL, Yang L, Li X, Kuang J, *et al.* ART1 silencing enhances apoptosis of mouse CT26 cells via the PI3K/Akt/NF- κ B pathway. *Cellular Physiology and Biochemistry*. 2013; 32: 1587–1599.
- [21] Liu Y, Jiang Z, Yang H, Yuan J, Zeng J, Wu J, *et al.* Gui Shao Tea Extracts Inhibit Gastric Cancer Growth in Vitro and in Vivo and Prolong Survival in Nude Mice. *Frontiers in Bioscience-Landmark*. 2022; 27: 250.
- [22] Tang Y, Wang YL, Yang L, Xu JX, Xiong W, Xiao M, *et al.* Inhibition of arginine ADP-ribosyltransferase 1 reduces the expression of poly (ADP-ribose) polymerase-1 in colon carcinoma. *International Journal of Molecular Medicine*. 2013; 32: 130–136.
- [23] Kuang J, Wang YL, Xiao M, Tang Y, Chen WW, Song GL, *et al.* Synergistic effect of arginine-specific ADP-ribosyltransferase 1 and poly (ADP-ribose) polymerase-1 on apoptosis induced by cisplatin in CT26 cells. *Oncology Reports*. 2014; 31: 2335–2343.
- [24] Ismail A, Ayala-Lopez N, Ahmad M, Watts SW. 3T3-L1 cells and perivascular adipocytes are not equivalent in amine transporter expression. *FEBS Letters*. 2017; 591: 137–144.
- [25] Sun N, Yang G, Zhao H, Savelkoul HFJ, An L. Multidose streptozotocin induction of diabetes in BALB/c mice induces a dominant oxidative macrophage and a conversion of TH1 to TH2 phenotypes during disease progression. *Mediators of Inflammation*. 2005; 2005: 202–209.
- [26] Luippold G, Beilharz M, Mühlbauer B. Chronic renal denervation prevents glomerular hyperfiltration in diabetic rats. *Nephrology, Dialysis, Transplantation*. 2004; 19: 342–347.
- [27] Dias LD, Casali KR, Leguisamo NM, Azambuja F, Souza MS, Okamoto M, *et al.* Renal denervation in an animal model of diabetes and hypertension: impact on the autonomic nervous system and nephropathy. *Cardiovascular Diabetology*. 2011; 10: 33.
- [28] Lee CK, Park KK, Lim SS, Park JHY, Chung WY. Effects of the licorice extract against tumor growth and cisplatin-induced toxicity in a mouse xenograft model of colon cancer. *Biological & Pharmaceutical Bulletin*. 2007; 30: 2191–2195.
- [29] Carlsson G, Gullberg B, Hafström L. Estimation of liver tumor volume using different formulas - an experimental study in rats. *Journal of Cancer Research and Clinical Oncology*. 1983; 105: 20–23.
- [30] Chen W, Chang Y, He L, Jian X, Li L, Gao L, *et al.* Effect of renal sympathetic denervation on hepatic glucose metabolism and blood pressure in a rat model of insulin resistance. *Journal of Hypertension*. 2016; 34: 2465–2474.
- [31] Katayama T, Sueta D, Kataoka K, Hasegawa Y, Koibuchi N, Toyama K, *et al.* Long-term renal denervation normalizes disrupted blood pressure circadian rhythm and ameliorates cardiovascular injury in a rat model of metabolic syndrome. *Journal of the American Heart Association*. 2013; 2: e000197.
- [32] Zhao L, Xu J, Liang F, Li A, Zhang Y, Sun J. Effect of Chronic Psychological Stress on Liver Metastasis of Colon Cancer in Mice. *PLoS ONE*. 2015; 10: e0139978.
- [33] Jansen L, Below J, Chang-Claude J, Brenner H, Hoffmeister M. Beta blocker use and colorectal cancer risk: population-based case-control study. *Cancer*. 2012; 118: 3911–3919.
- [34] Hopp AK, Gruter P, Hottiger MO. Regulation of Glucose Metabolism by NAD(+) and ADP-Ribosylation. *Cells*. 2019; 8: 890.
- [35] de Lima-Seolin BG, Nemecek-Bakk A, Forsyth H, Kirk S, da Rosa Araujo AS, Schenkel PC, *et al.* Bucindolol Modulates Cardiac Remodeling by Attenuating Oxidative Stress in H9c2 Cardiac Cells Exposed to Norepinephrine. *Oxidative Medicine and Cellular Longevity*. 2019; 2019: 6325424.
- [36] Elek Z, Rónai Z, Keszler G, Harsányi L, Kontsek E, Herold Z, *et al.* Correlation between Expression Profiles of Key Signaling Genes in Colorectal Cancer Samples from Type 2 Diabetic and Non-Diabetic Patients. *Life*. 2020; 10: 216.
- [37] Burgeiro A, Cerqueira MG, Varela-Rodríguez BM, Nunes S, Neto P, Pereira FC, *et al.* Glucose and Lipid Dysmetabolism in a Rat Model of Prediabetes Induced by a High-Sucrose Diet. *Nutrients*. 2017; 9: 638.
- [38] Khadke SP, Kuvalekar AA, Harsulkar AM, Mantri N. High Energy Intake Induced Overexpression of Transcription Factors and Its Regulatory Genes Involved in Acceleration of Hepatic Lipogenesis: A Rat Model for Type 2 Diabetes. *Biomedicines*. 2019; 7: 76.
- [39] Magalhães DAD, Kume WT, Correia FS, Queiroz TS, Allebrandt Neto EW, Santos MPD, *et al.* High-fat diet and streptozotocin in the induction of type 2 diabetes mellitus: a new proposal. *Anais Da Academia Brasileira De Ciencias*. 2019; 91: e20180314.